



## Cytotoxicity and DNA binding property of phenanthrene imidazole with polyglycol side chains

Shuxiang Wang<sup>a,b</sup>, Hongdong Li<sup>a</sup>, Chao Chen<sup>a</sup>, Jinchao Zhang<sup>a,b,\*</sup>, Shenghui Li<sup>a,b</sup>, Xinying Qin<sup>a</sup>, Xiaoliu Li<sup>a,b,\*</sup>, Kerang Wang<sup>a</sup>

<sup>a</sup> Chemical Biology Key Laboratory of Hebei Province, College of Chemistry and Environmental Science, Hebei University, Baoding 071002, China

<sup>b</sup> Key Laboratory of Medicinal Chemistry and Molecular Diagnosis of Ministry of Education, Hebei University, Baoding 071002, China

### ARTICLE INFO

#### Article history:

Received 1 June 2012

Revised 17 August 2012

Accepted 21 August 2012

Available online 30 August 2012

#### Keywords:

Phenanthrene imidazole derivatives

Polyglycol side chain

Binding property

Cytotoxicity

### ABSTRACT

A series of phenanthrene imidazole with polyglycol side chain (**2a–2c** and **3a–3c**) were synthesized and characterized by IR, NMR and MS. The cytotoxicity of **2a–2c** and **3a–3c** against cancer cell lines (HL-60, BGC-823, Bel-7402 and KB) in vitro were measured using MTT method. The DNA binding properties of **3a–3c** were investigated by UV, fluorescence, CD spectroscopies and thermal denaturation. The results indicate that **2a** exhibits higher cytotoxicity than cisplatin against BGC-823 and Bel-7402 cell lines, **3b** and **3c** exhibit higher cytotoxicity than **2b** and **2c** against BGC-823, Bel-7402 and KB cell lines. The cytotoxic effect of **2a–2c** decrease with the increase of side chains length, the cytotoxic effect of **3a–3c** increased with the increasing length of side chains against BGC-823, Bel-7402 and KB cell lines. Compounds **3a–3c** intercalated DNA with a vertical orientation in the intercalation pocket. The binding constants of **3a–3c** with Ct-DNA are  $1.68 \times 10^6$ ,  $1.51 \times 10^6$  and  $0.709 \times 10^6 \text{ M}^{-1}$ , respectively. The binding affinity of **3a–3c** with Ct-DNA trended to decrease with the increasing length of polyglycol side chains.

© 2012 Elsevier Ltd. All rights reserved.

In recent years, studies on the small molecule DNA binding agents towards their application on various biological responses particularly anticancer activity is an active area of research.<sup>1,2</sup> Various types of interaction of these small molecules with DNA have been known. An electrostatic interaction that extends the negatively charged phosphates outside the DNA double helix, interaction with grooves of DNA, and intercalation model in which the base pairs of DNA unwind to accommodate the intercalating agent are some important binding modes. These binding interactions with DNA are of interest in the development of drugs, new biochemical tools, etc. Phenanthrene imidazole showed favorable properties such as stability, ease of synthesis, a high extinction coefficient and tuneable absorption and emission properties,<sup>3</sup> which was commonly utilized in optical sensors and probes, such as *endo/exo*-11-(4-(1*H*-phenanthro[9,10-*d*]imidazol-2-yl)phenoxy)undecylbicyclo [2.2.1] hept-5-ene-2-carboxylat (**A**) and 2-[4-(diphenylamino) phenyl]-1*H*-phenanthro[9,10-*d*]imidazole (**B**) (Fig. 1). Cote et al.<sup>4</sup> designed and synthesized a series of substituted phenanthrene imidazoles as anti-inflammatory and analgesic. Compound **MF63** (Fig. 1) has been identified as a novel potent, selective and orally active mPGES-1 inhibitor and exhibited a significant analgesic effect with dosed at 30 and 100 mg/kg.

As far as we know, phenanthrene imidazole was rare as anticancer agent. Here, we design and synthesize a series of phenanthrene imidazole derivatives. These compounds contain a different length of polyglycol side chains and a planar chromophore. The polyglycol side chains can form H-bonds with biomacromolecules by the –OH groups, which may increased the binding affinity between compounds and DNA,<sup>5–7</sup> and the planar of phenanthrene imidazole may insert into two base pairs in the DNA helix, resulting in mis-coding and possible cell death.<sup>8</sup>

As shown in Scheme 1, compounds **2a–2c** were synthesized by condensation reaction of 5,6-phenanthrenequinone with various 4-(polyglycol)-benzaldehyde and  $\text{NH}_4\text{OAc}$  in acetic acid.<sup>3</sup> Compounds **3a–3c** were obtained by methylation reaction of **2a–2c**. All of them were characterized by IR, NMR and MS spectrometry.<sup>9</sup> The cytotoxicity of **2a–2c** and **3a–3c** were preliminarily evaluated against different tumor cell lines, including HL-60 (immature granulocyte leukemia), Bel-7402 (liver carcinoma), BGC-823 (gastrocarcinoma) and KB (nasopharyngeal carcinoma). It is well known that

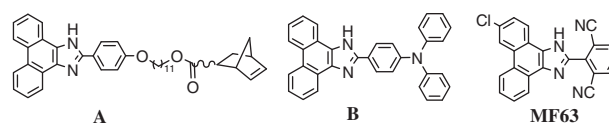
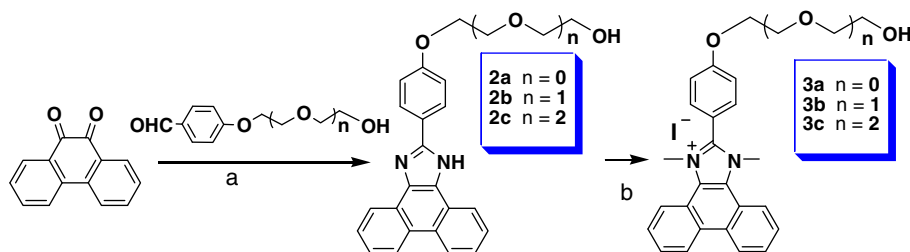


**Figure 1.** Phenanthrene imidazole derivatives in optical sensors and anti-inflammatory.

\* Corresponding authors. Tel./fax: +86 312 507 9005 (J.Z.); tel./fax: +86 312 597 1116 (X.L.).

E-mail addresses: jczhang6970@yahoo.com.cn (J. Zhang), wsxhbu6564@126.com, lixl@hbu.edu.cn (X. Li).



**Scheme 1.** The route of synthesis **2a–2c** and **3a–3c** (a) HOAc, NH<sub>4</sub>OAc, reflux, 3 h; (b) THF, CH<sub>3</sub>I, reflux, 20 h.

the DNA phosphoric acid skeleton is negatively charged with electricity. The compounds **3a–3c** have a net positive charge due to N-methylation, which enhance their water-solubility and may enhance the binding affinity of **3a–3c** with DNA. So compounds **3a–3c** were selected to explore the binding affinity with calf thymus DNA (ct-DNA).

The cytotoxicity of phenanthrene imidazole derivatives **2a–2c** and **3a–3c** against HL-60, BGC-823, Bel-7402 and KB cell lines in vitro were measured with MTT (3-(4,5-dimethylthiazol-2-yl)-2,5-diphenyltetrazolium bromide) method. As shown in Table 1, most compounds showed lower IC<sub>50</sub> values (<30 μM) and exerted cytotoxic effects with selectivity against tested carcinoma cell lines. Compound **2a** with the side chain of 4-(2-hydroxy-glycol)-phenyl exhibited potent cytotoxicity against BGC-823 and Bel-7402 cell lines with the IC<sub>50</sub> values of 6.36 and 4.65 μM, which was better than that of positive control drug (cisplatin). The order of IC<sub>50</sub> value of **2a–2c** were **2c** > **2b** > **2a** against BGC-823, Bel-7402 and KB cell lines, indicating that the cytotoxic effect of **2a–2c** decreases with the increase of side chains length. Although, the cytotoxicity of **3a** have some decrease comparing with that of **2a**, compounds **3b** and **3c** showed obviously enhanced cytotoxicity comparing with that of **2b** and **2c** against BGC-823, Bel-7402 and KB cell lines. Compound **3c** exhibited the best cytotoxicity against BGC-823, Bel-7402 and KB cell lines among the compounds **3a–3c**. The order of IC<sub>50</sub> value of **3a–3c** were **3a** > **3b** > **3c** against BGC-823, Bel-7402 and KB cell lines, indicating that the cytotoxic effect of **3a–3c** enhanced with the increase of side chains length.

In addition to cytotoxicity study, the DNA binding properties were investigated by UV-vis, fluorescence, circular dichroism (CD) spectroscopy and DNA thermal denaturation experiment. Since compounds **2a–2c** exhibit poor solubility in buffer solution and can be dissolved only in a few solvents such as DMSO and DMF, we selected compounds **3a–3c** as the DNA binders to detect the binding properties of **3a–3c** with Ct-DNA.

The DNA binding properties of **3a–3c** with Ct-DNA were investigated by UV-vis spectra in phosphate buffer (1 mM, pH 7.5) containing 20 mM NaCl, 5% DMSO (volume ratio) at 25 °C. The maximum absorption intensity of **3a–3c** overlapped with Ct-DNA at about 260 nm, so the absorption wavelength was selected at 300–400 nm to eliminate the interference of Ct-DNA. As shown in Figure 2, the absorption intensity of **3a–3c** decreased with the increasing concentrations of Ct-DNA, and the maximum absorption

peaks show obvious hypochromicity and bathochromic shift (Table 2), which implies that **3a–3c** may insert into the base pairs of DNA as DNA-intercalating agents.<sup>10</sup> Using the nonlinear least-squares curve fitting method<sup>11</sup> by fitting the experimental data of the maximum absorption changes, the binding constants of **3a–3c** with Ct-DNA were obtained to be  $1.68 \times 10^6$ ,  $1.51 \times 10^6$  and  $0.709 \times 10^6$  M<sup>-1</sup>, respectively, which suggested that the length of the side chains had slight influenced on the DNA binding properties and indicated that the binding affinity trended to decrease with the increasing length of polyglycol side chains for the tested compounds. For compounds **3a–3c**, though the DNA binding affinity decreased, the cytotoxicity enhanced with the increase of the length of the polyglycol side chain may be the polyglycol side chain improves the solubility of phenanthrene imidazoles.

The fluorescence properties were performed to investigate the interactions between **3a–3c** and Ct-DNA in phosphate buffer (1 mM, pH 7.5) containing 20 mM NaCl, 5% DMSO at 25 °C. As shown in Figure 3, the fluorescence spectra of **3a–3c** show a broad emission band around 400 nm. Upon addition of Ct-DNA, the fluorescence emission intensity of **3a–3c** decreases due to forming the complex between Ct-DNA and compounds and changing the molecular rearrangements and energy transfer.<sup>12</sup> Furthermore, the maximum emission bands are blue shifted by about 3 nm, which implies that the phenanthrene imidazole backbones of **3a–3c** enter Ct-DNA-stacking region with low polarity.<sup>13,14</sup> These spectral characteristic also indicated that **3a–3c** intercalated into the bases of the Ct-DNA.<sup>15,16</sup> The observed fluorescence intensities were quantified by plotting  $F/F_0$  as a function of Ct-DNA concentrations, where  $F_0$  and  $F$  are the fluorescence intensity without and with Ct-DNA, respectively. Stern-Volmer analysis<sup>17</sup> gives insight into the efficiency of fluorescence reduction of **3a–3c** with the increasing concentrations of Ct-DNA, which are calculated<sup>18,19</sup> as  $9.95 \times 10^3$ ,  $9.88 \times 10^3$  and  $6.61 \times 10^3$  M<sup>-1</sup> (Fig. 3, inset), respectively, which indicate that the fluorescence of **3a–3c** are sensitive to the Ct-DNA concentrations. This result was in agreement with the UV-vis analysis.

CD is a useful technique to investigate the conformational changes in DNA morphology during small molecules-DNA interactions. As shown in Figure 4, the CD spectrum of free Ct-DNA showed a negative band at 247 nm due to the polynucleotide helicity, and a positive band at 277 nm due to the base stacking, which indicated that the Ct-DNA existed in the right-band B form.<sup>20,21</sup> Upon addition of compounds **3a–3c**, the intensity of the positive band increases at 277 nm and without significant wavelength change. Additionally, weak positive induced circular dichroisms (ICD) signals were observed in the region of the characteristic absorption of the phenanthrene imidazole derivatives (350–500 nm), which indicated that **3a–3c** intercalated DNA with a vertical orientation in the intercalation pocket.<sup>22</sup>

Additional evidence for intercalation into the DNA was obtained from thermal denaturation studies. It is well known that the double-helical structure of DNA is very stable due to hydrogen bonding and base stacking interactions. When heating, the double helix

**Table 1**  
Cytotoxicity data for **3a–3c** (IC<sub>50</sub> ± SD, μM)

Compound	BGC-823	Bel-7402	KB	HL-60
<b>2a</b>	6.36 ± 0.34	4.65 ± 0.16	7.03 ± 0.46	11.28 ± 0.89
<b>2b</b>	22.47 ± 0.83	18.11 ± 0.73	30.69 ± 0.94	8.14 ± 0.67
<b>2c</b>	24.21 ± 0.91	27.95 ± 0.82	44.62 ± 0.84	11.93 ± 0.78
<b>3a</b>	10.74 ± 0.75	14.07 ± 0.75	14.45 ± 0.71	24.83 ± 0.87
<b>3b</b>	9.35 ± 0.69	10.74 ± 0.63	10.95 ± 0.68	12.10 ± 0.76
<b>3c</b>	7.01 ± 0.47	10.55 ± 0.77	9.12 ± 0.72	15.63 ± 0.85
Cisplatin	6.48 ± 0.24	8.12 ± 0.20	2.65 ± 0.33	2.89 ± 0.18

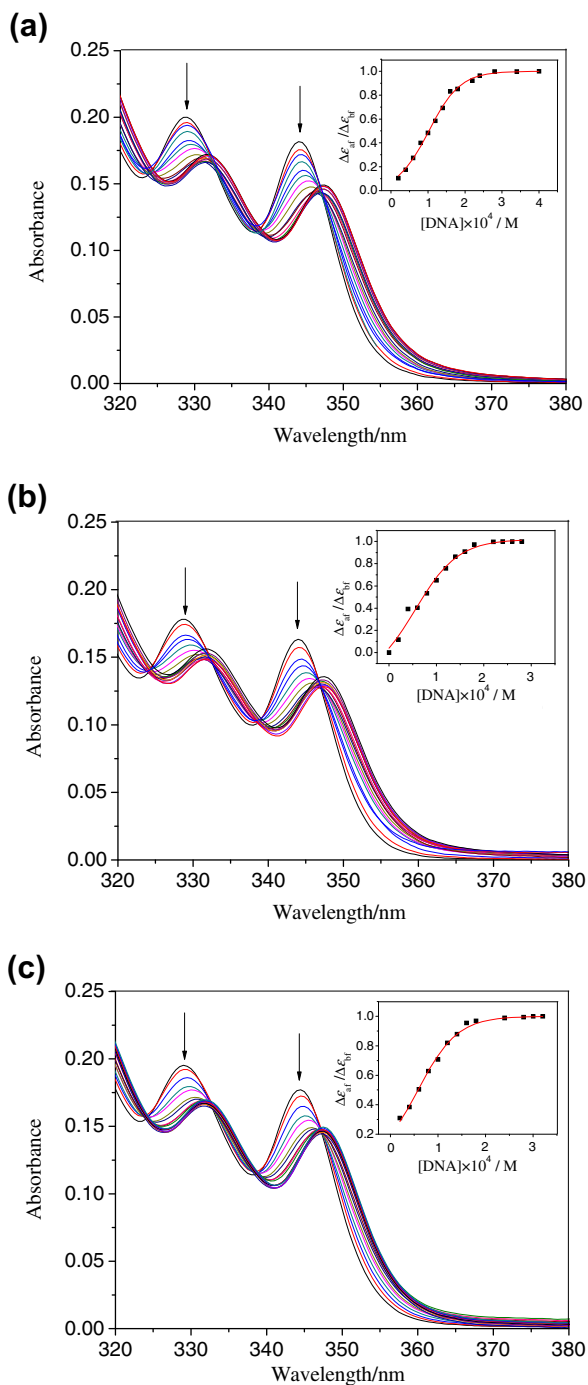


**Figure 2.** UV-vis spectra of **3a–3c** in the absence and presence of Ct-DNA. UV-vis spectra of **3a** (a), **3b** (b) and **3c** (c) at the concentration of  $4.0 \times 10^{-5}$  M upon addition of Ct-DNA (arrow: 0–400  $\mu$ M for **3a–3c**) in phosphate buffer (1 mM, pH 7.5) containing 20 mM NaCl, 5% DMSO at 25 °C. Inset: the fitting plots of the binding constants for **3a–3c** with Ct-DNA obtained at the maximum absorption band.

**Table 2**  
Binding constants (*K*) and photometric properties of **3a–3c** with Ct-DNA

Compound	Hypochromicity <sup>a</sup> (%)	Bathochromic shift <sup>a</sup> (nm)	<i>K</i> ( $M^{-1} \text{ cm}^{-1}$ )
<b>3a</b>	21.2	3.5	$1.68 \times 10^6$
<b>3b</b>	21.7	3.5	$1.51 \times 10^6$
<b>3c</b>	26.4	3.0	$0.709 \times 10^6$

<sup>a</sup> Obtained at  $\lambda_{\text{max}}$ .

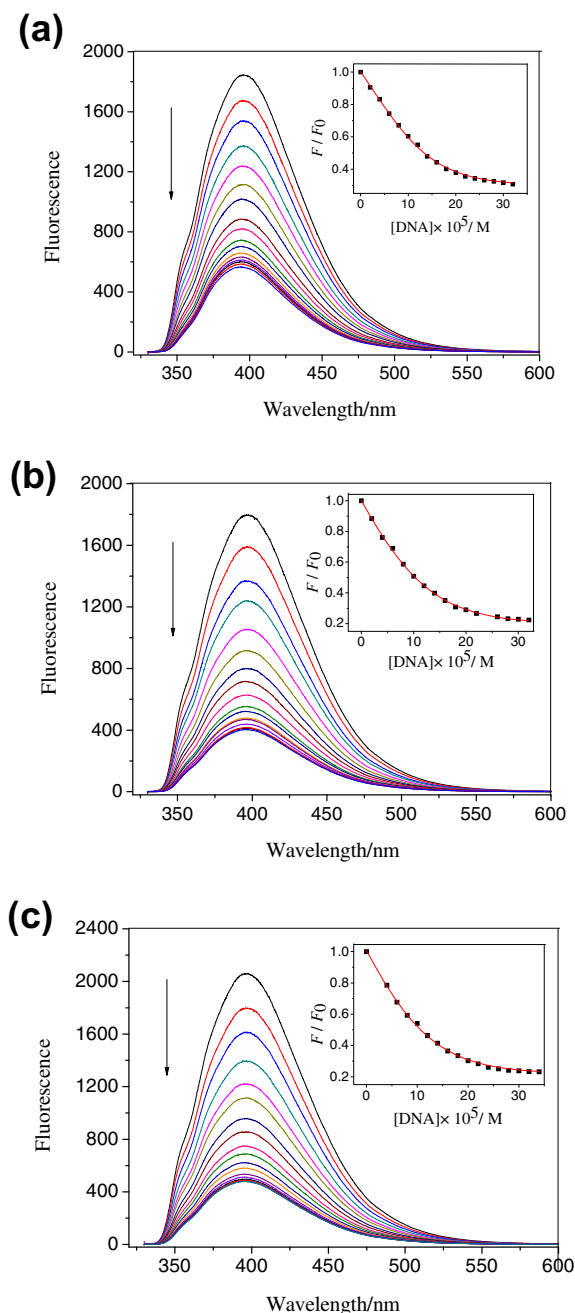


**Figure 3.** Fluorescence spectral of **3a–3c** in the absence and presence of Ct-DNA. Fluorescence spectral changes of **3a** (a,  $\lambda_{\text{ex}} = 320$  nm), **3b** (b,  $\lambda_{\text{ex}} = 320$  nm) and **3c** (c,  $\lambda_{\text{ex}} = 320$  nm) at the concentration of  $4.0 \times 10^{-5}$  M upon addition of Ct-DNA (arrow: 0–400  $\mu$ M) in phosphate buffer (1 mM, pH 7.5) containing 20 mM NaCl, 5% DMSO at 25 °C. The excitation slit width and emission slit width are 5.0 nm. Inset: Stern-Volmer plots for the observed fluorescence decrease on addition of Ct-DNA to phenanthrene imidazole derivatives.

dissociates into single strands due to the breaking of hydrogen bonding and stacking interactions. The temperature, at which a half of a DNA sample is melted, is known as the melting temperature ( $T_m$ ). A change of  $T_m$  may be observed if a molecule binds with DNA.<sup>23</sup> Thus the thermal behavior of DNA in the presence of phenanthrene imidazole derivatives provides useful information on the conformational changes and the strength of the DNA-compound complexes. The melting curves of Ct-DNA in the absence and presence of **3a–3c** are illustrated in Figure 5 and Table 3, respectively. The  $T_m$  value for the free Ct-DNA is 68.7 °C. Upon addition of **3a–**

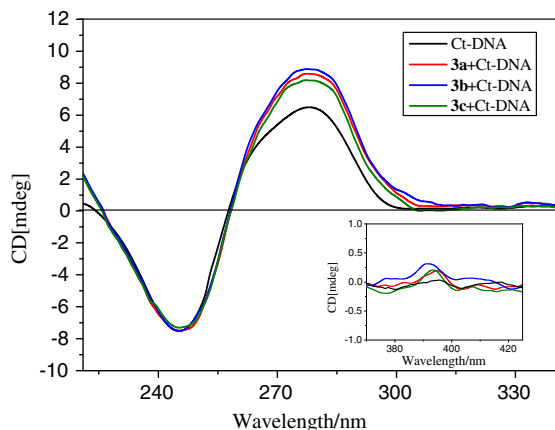


**Figure 4.** CD spectral of Ct-DNA in the absence and presence of **3a–3c** CD spectra of Ct-DNA ( $6.0 \times 10^{-5}$  M) and in presence of **3a–3c** ( $2.0 \times 10^{-5}$  M) in phosphate buffer (10 mM, pH 7.5) containing 20 mM NaCl, 5% DMSO at 25 °C.

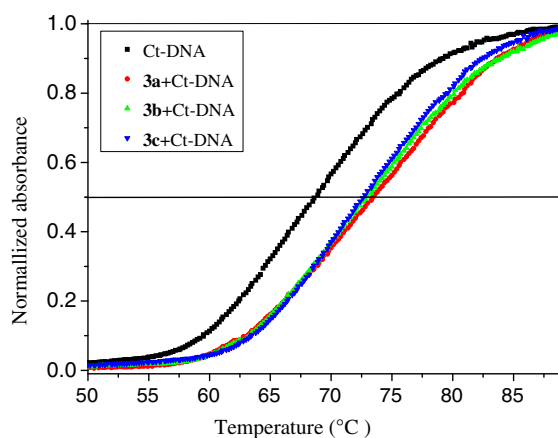


**Figure 5.** DNA melting curves for Ct-DNA in the absence and presence of **3a–3c** DNA melting curves for Ct-DNA ( $5.0 \times 10^{-5}$  M) (■) and in presence of **3a** (◆), **3b** (▲) and **3c** (▼) with concentration of  $5.0 \times 10^{-6}$  M in phosphate buffer (1 mM, pH 7.5) containing 2 mM NaCl, 5% DMSO.

**Table 3**

Average  $T_m$  and  $\Delta T_m$  for Ct-DNA in the absence and in presence of **3a–3c**

Compound	$T_m$ (°C)	$\Delta T_m$ (°C)
Ct-DNA	68.7	—
<b>3a</b>	73.5	4.8
<b>3b</b>	72.9	4.2
<b>3c</b>	72.7	4.0

**3c**, obvious changes in the DNA melting temperature were observed. The  $T_m$  values increased to 73.5, 72.9 and 72.7 °C, respectively, indicating that the insertion of compounds enhanced the stability of the DNA double helix conformation and increased the DNA melting temperature. The level of the increased melting temperature ( $\Delta T_m$ ) induced by DNA–compound interactions is 4.8, 4.2 and 4.0 °C, respectively. Compounds **3b** and **3c** possessed lower DNA melting temperature than **3a**. The result was in agreement with the UV–vis and fluorescence analysis.

In conclusion, a series of novel phenanthrene imidazole derivatives with various polyglycol side chains were synthesized by condensation and N-methylation reactions. The phenanthrene imidazole derivatives showed cytotoxic effects with selectivity against tested carcinoma cell lines. Compounds **2a** and **3c** exhibit better cytotoxicity against BGC-823, Bel-7402 and KB cell lines.

Furthermore, the binding properties of **3a–3c** with Ct-DNA were investigated by UV–vis, fluorescence and CD spectra and thermal denaturation experiment. The results showed that compounds **3a–3c** intercalated DNA with a vertical orientation in the intercalation pocket. The binding constants of **3a–3c** with Ct-DNA are  $1.68 \times 10^6$ ,  $1.51 \times 10^6$  and  $0.709 \times 10^6$  M<sup>-1</sup>, respectively. The binding affinity of **3a–3c** with Ct-DNA trended to decrease with the increasing length of polyglycol side chains.

## Acknowledgments

This work was supported by the National Basic Research 973 Program (No. 2010CB534913), the Special Foundation for State Major New Drug Research Program of China (No. 2009ZX09103-139), the Natural Science Foundation of Hebei Province (No. B2011201135), the Nature Science Foundation for Distinguished Young Scholars of Hebei Province (No. B2011201164), the Key Basic Research Special Foundation of Technology Ministry of Hebei Province (Grant No. 11966412D), the Key Research Project Foundation of Department of Education of Hebei Province (No. ZD2010142), the Technology Research and Development Foundation of Hebei Province (No. 11276431), the Joint Research Foundation of the Natural Science Foundation of Hebei Province and China Shiyao Pharmaceutical Group Co., Ltd. (B2011201174).

## References and notes

- Demeunynck, M.; Bailly, C.; Wilson, W. D. *DNA and RNA Binders: From Synthesis to Nucleic Acid Complexes*; Wiley-VCH: Weinheim, 2003.
- Tiekink, E. R. T.; Gielen, M. *Metallotherapeutic Drugs and Metal-based Diagnostic Agents: The Use of Metals in Medicine*; John Wiley & Sons, 2005.
- Steck, E. A.; Day, A. R. *J. Am. Chem. Soc.* **1943**, 65, 452.
- Côté, B.; Boulet, L.; Brideau, C.; Claveau, D.; Ethier, D.; Frenette, R.; Gagnon, M.; Giroux, A.; Guay, J.; Guiral, S.; Mancini, J.; Martins, E.; Massé, F.; Méthot, N.; Riendeau, D.; Rubin, J.; Xu, D.; Yu, H.; Ducharme, Y.; Friesen, R. W. *Bioorg. Med. Chem. Lett.* **2007**, 17(24), 6816.
- Huang, T.; Wang, X. D.; Wei, Y. B.; Huang, S. L.; Huang, Z. S.; Tan, J. H.; An, L. K.; Wu, J. Y.; Chan, A. S. C.; Gu, L. Q. *Eur. J. Med. Chem.* **2008**, 43, 973.
- Ruchelman, A. L.; Singh, S. K.; Ray, A.; Wu, X. H.; Yang, J. M.; Li, T. K.; Liu, A.; Leroy, F.; Liu, L. F.; LaVoie, E. J. *Bioorg. Med. Chem.* **2003**, 11, 2061.
- Van der Graaf, W.; Vries, E. D. *Anticancer Drugs* **1990**, 1, 109.
- Kamal, A.; Ramu, R.; Khanna, G. B. R.; Saxena, A. K.; Shanmugavel, M.; Pandita, R. M. *Bioorg. Med. Chem. Lett.* **2004**, 14(19), 4907.
- 2a**: A light yellow solid; yield: 70.2%; mp >250 °C; IR (KBr, cm<sup>-1</sup>): 3520 (O–H), 3311 (N–H), 3062–3008 (C–H, Ph), 1150–1060 (C–O–C). <sup>1</sup>H NMR (600 MHz, DMSO-d<sub>6</sub>, TMS): δ (ppm) 8.85 (d, *J* = 8.3 Hz, 2H, ArH), 8.63 (d, *J* = 6.9 Hz, 2H, ArH), 8.33 (d, *J* = 8.8 Hz, 2H, ArH), 7.72 (t, *J* = 7.5 Hz, 2H, ArH), 7.62 (t, *J* = 7.0 Hz, 2H, ArH), 7.15 (d, *J* = 8.8 Hz, 2H, ArH), 4.11 (t, *J* = 5.0 Hz, 2H, CH<sub>2</sub>), 3.78 (t, *J* = 4.7 Hz, 2H, CH<sub>2</sub>), <sup>13</sup>C NMR (150 MHz, DMSO-d<sub>6</sub>) δ (ppm) 60.03, 70.16, 115.25, 122.52, 123.52, 123.52, 125.44, 127.44, 127.86, 128.32, 149.85, 160.06. MS (ESI) *m/z*: 355.1 [M+H]<sup>+</sup>. **2b**: A yellow solid; yield: 84.5%; mp >250 °C; IR (KBr, cm<sup>-1</sup>): 3680 (O–H), 3280 (N–H), 3032–3008 (C–H, Ph), 1150–1060 (C–O–C). <sup>1</sup>H NMR (600 MHz, DMSO-d<sub>6</sub>, TMS): δ (ppm) 8.85 (d, *J* = 8.3 Hz, 2H, ArH), 8.61 (d, *J* = 6.7 Hz, 2H, ArH), 8.30 (d, *J* = 8.7 Hz, 2H, ArH), 7.72 (t, *J* = 7.5 Hz, 2H, ArH), 7.62 (t, *J* = 7.6 Hz, 2H, ArH), 7.17 (d, *J* = 8.7 Hz, 2H, ArH), 4.22 (t, *J* = 9.0 Hz, 2H, CH<sub>2</sub>), 3.8 (t, *J* = 9.0 Hz, 2H, CH<sub>2</sub>), 3.54 (t, *J* = 3.3 Hz, 4H, CH<sub>2</sub>), <sup>13</sup>C NMR (150 MHz, DMSO-d<sub>6</sub>) δ (ppm) 60.73, 67.87, 69.39, 70.98, 115.27, 122.46, 123.68, 125.44, 127.51, 127.95, 128.21, 149.83, 159.85. MS (ESI) *m/z*: 399.2 [M+H]<sup>+</sup>. **2c**: A white solid; yield: 82.5%; mp >250 °C; IR (KBr, cm<sup>-1</sup>): 3500 (O–H), 3301 (N–H), 3020–3008 (C–H, Ph), 1150–1060 (C–O–C). <sup>1</sup>H NMR (600 MHz, DMSO-d<sub>6</sub>, TMS): δ (ppm) 8.98 (d, *J* = 8.4 Hz, 2H, ArH), 8.64 (d, *J* = 7.9 Hz, 2H, ArH), 8.28 (d, *J* = 8.8 Hz, 2H, ArH), 7.88 (t, *J* = 7.5 Hz, 2H, ArH), 7.80 (t, *J* = 7.6 Hz, 2H, ArH), 7.36 (d, *J* = 8.7 Hz, 2H, ArH), 4.29 (t, *J* = 8.4 Hz, 2H, CH<sub>2</sub>), 3.84 (t, *J* = 9.0 Hz, 2H, CH<sub>2</sub>), 3.65 (t, *J* = 9.6 Hz, 2H, CH<sub>2</sub>), 3.58 (t, *J* = 9.6 Hz, 2H, CH<sub>2</sub>), 3.51 (t, *J* = 10.2 Hz, 2H, CH<sub>2</sub>), 3.46 (t, *J* = 10.8 Hz, 2H, CH<sub>2</sub>), <sup>13</sup>C NMR (150 MHz, DMSO-d<sub>6</sub>) δ (ppm) 60.7, 67.81, 69.40, 70.27, 70.48, 72.86, 115.34, 122.33, 123.58, 125.51, 127.50, 127.94, 128.20, 149.76, 159.89. MS (ESI) *m/z*: 443.2 [M+H]<sup>+</sup>. **3a**: An orange solid; yield: 31.9%; mp >250 °C; IR (KBr, cm<sup>-1</sup>): 3520 (O–H), 3042–3012 (C–H, Ph), 1100–1040 (C–O–C). <sup>1</sup>H NMR (600 MHz, DMSO-d<sub>6</sub>, TMS): δ (ppm) 9.11 (d, *J* = 9.2 Hz, 2H, ArH), 8.76 (d, *J* = 9.1 Hz, 2H, ArH), 7.92–7.89 (m, 4H, ArH), 7.84 (d, *J* = 8.6 Hz, 2H, ArH), 7.38 (d, *J* = 8.6 Hz, 2H, ArH), 4.27 (s, 6H, CH<sub>3</sub>), 4.19 (t, *J* = 4.7 Hz, 2H, CH<sub>2</sub>), 3.80 (t, *J* = 4.4 Hz, 2H, CH<sub>2</sub>), <sup>13</sup>C NMR (150 MHz, DMSO-d<sub>6</sub>) δ (ppm) 38.3, 40.5, 59.9, 70.6, 113.3, 116.2, 120.8, 121.2, 123.1, 125.2, 126.6, 128.5, 129.0, 129.8, 133.7, 149.8, 162.5; MS (ESI) *m/z*: 383.2 [M–I]<sup>+</sup>. **3b**: A brown solid; yield: 40.3%; mp >250 °C; IR (KBr, cm<sup>-1</sup>): 3500 (O–H), 3069–3008 (C–H, Ph), 1100–1040 (C–O–C). <sup>1</sup>H NMR (600 MHz, DMSO-d<sub>6</sub>, TMS): δ (ppm) 9.12 (d, *J* = 9.6 Hz, 2H, ArH), 8.77 (d, *J* = 9.4 Hz, 2H, ArH), 7.92–7.90 (m, 4H, ArH), 7.84 (d, *J* = 8.7 Hz, 2H, ArH), 7.39 (d, *J* = 8.8 Hz, 2H, ArH), 4.31 (t, *J* = 9.0 Hz, 2H,

- CH<sub>2</sub>), 4.27 (s, 6H, CH<sub>3</sub>), 3.85 (t, *J* = 9.0 Hz, 2H, CH<sub>2</sub>), 3.56 (t, *J* = 3.0 Hz, 4H, CH<sub>3</sub>). <sup>13</sup>C NMR (150 MHz, DMSO-*d*<sub>6</sub>) δ (ppm) 38.3, 40.5, 60.7, 68.3, 69.2, 73.0, 113.4, 116.2, 121.2, 123.1, 125.3, 126.6, 128.5, 129.0, 129.8, 133.7, 149.7, 162.3. MS (ESI) *m/z*: 427.2 [M–I]<sup>+</sup>. **3c**: A yellow solid; yield: 37.6%; mp >250 °C; IR (KBr, cm<sup>-1</sup>): 3505 (O–H), 3072–3002 (C–H, Ph), 1100–1040 (C–O–C). <sup>1</sup>H NMR (600 MHz, DMSO-*d*<sub>6</sub>, TMS): δ (ppm) 9.14 (d, *J* = 9.7 Hz, 2H, ArH), 8.79 (d, *J* = 9.5 Hz, 2H, ArH), 7.94–7.91 (m, 4H, ArH), 7.85 (d, *J* = 8.7 Hz, 2H, ArH), 7.41 (d, *J* = 8.7 Hz, 2H, ArH), 4.30 (t, *J* = 9.0 Hz, 2H, CH<sub>2</sub>), 4.29 (s, 6H, CH<sub>3</sub>), 3.85 (t, *J* = 9.0 Hz, 2H, CH<sub>2</sub>), 3.65 (t, *J* = 9.6 Hz, 2H, CH<sub>2</sub>), 3.58 (t, *J* = 9.6 Hz, 2H, CH<sub>2</sub>), 3.51 (t, *J* = 9.6 Hz, 2H, CH<sub>2</sub>), 3.46 (t, *J* = 5.2 Hz, 2H, CH<sub>2</sub>). <sup>13</sup>C NMR (150 MHz, DMSO-*d*<sub>6</sub>) δ (ppm) 38.3, 40.6, 60.7, 68.3, 69.3, 70.3, 70.5, 72.9, 113.4, 116.2, 121.2, 123.1, 125.3, 126.6, 128.5, 129.0, 129.8, 133.7, 149.7, 162.3. MS (ESI) *m/z*: 471.2 [M–I]<sup>+</sup>.
- Long, E. C.; Barton, J. K. *Acc. Chem. Res.* **1990**, *23*, 271.
  - Kozurkova, M.; Sabolova, D.; Paulikova, H.; Janovec, L.; Kristian, P.; Bajdichova, M.; Buša, J.; Podhradsky, D.; Imrich, J. *Int. J. Biol. Macromol.* **2007**, *41*, 415.
  - Krishnamoorthy, P.; Sathyadevi, P.; Cowley, A. H.; Dharmaraj, N. *Eur. J. Med. Chem.* **2011**, *46*, 3376.
  - Yang, X.; Liu, W.; Jin, W.; Shen, G.; Yu, R. *Spectrochim. Acta A* **1999**, *55*, 2719.
  - Xie, L. J.; Xu, Y. F.; Wang, F.; Liu, J. W.; Qian, X. H.; Cui, J. N. *Bioorg. Med. Chem.* **2009**, *17*, 804.
  - Sahoo, D.; Bhattacharya, P.; Chakravorti, S. *J. Phys. Chem. B* **2010**, *114*, 2044.
  - Faulhaber, K.; Granzhan, A.; Ihmels, H.; Otto, D.; Thomas, L.; Wells, S. *Photochem. Photobiol. Sci.* **2011**, *10*, 1535.
  - Lakowicz, J. R. *Principles of Fluorescence Spectroscopy*; SPIE Digital Library: New York, 1983. 265.
  - Pandey, S.; Baker, G. A.; Kane, M. A.; Bonzagni, N. J.; Bright, F. V. *Langmuir* **2000**, *16*, 5593.
  - Wang, J.; Wang, D.; Miller, E. K.; Moses, D.; Bazan, G. C.; Heeger, A. J. *Macromolecules* **2000**, *33*, 5153.
  - Uma Maheswari, P.; Palaniandavar, M. *Inorg. Chim. Acta.* **2004**, *357*, 901.
  - Jiang, X.; Shang, L.; Wang, Z. X.; Dong, S. *J. Biophys. Chem.* **2005**, *118*, 42.
  - Zhang, Z. C.; Yang, Y. Y.; Zhang, D. N.; Wang, Y. Y.; Qian, X. H.; Liu, F. Y. *Bioorg. Med. Chem.* **2006**, *14*, 6962.
  - Chaveerach, U.; Meenongwa, A.; Trongpanich, Y.; Soikum, C.; Chaveerach, P. *Polyhedron* **2010**, *29*, 731.